Molecular Therapy
Nucleic Acids
Original Article

HIF1A-AS2 induces osimertinib resistance in lung adenocarcinoma patients by regulating the miR-146b-5p/IL-6/STAT3 axis

Jiahui Si,[1,3] Yuanyuan Ma,[2,3] Chao Lv,[2] Yang Hong,[2] Hongyu Tan,[1] and Yue Yang[2]

[1]Department of Anesthesiology, Key Laboratory of Carcinogenesis and Translational Research (Ministry of Education), Peking University Cancer Hospital and Institute, Beijing 100142, China; [2]Department of Thoracic Surgery II, Key Laboratory of Carcinogenesis and Translational Research (Ministry of Education), Peking University Cancer Hospital and Institute, Beijing 100142, China

Although epidermal growth factor receptor tyrosine kinase inhibitors (TKIs) show efficacy in lung adenocarcinoma (LUAD) patients, TKI resistance inevitably develops, limiting long-term results. Thus, there is an urgent need to address drug resistance in LUAD. Long non-coding RNA (lncRNA) HIF1A-AS2 could be a critical mediator in the progression of various tumor types. We examined the function of HIF1A-AS2 in modifying tumor aggravation and osimertinib resistance in lung adenocarcinoma. Using clinical samples, we showed that HIF1A-AS2 was upregulated in LUAD specimens, predicting poorer overall survival and disease-free survival. HIF1A-AS2 silencing inhibited the proliferation, migration, and tumorigenesis of LUAD cells and therapeutic efficacy of osimertinib against tumor cells *in vitro* and *in vivo*. RNA precipitation assays, western blotting, luciferase assays, and rescue experiments demonstrated that HIF1A-AS2 sponged microRNA-146b-5p (miR-146b-5p), promoting interleukin-6 (IL-6) expression, activating the IL-6/STAT3 pathway, and leading to LUAD progression. miR-146b-5p and IL-6 levels were correlated with the prognosis of LUAD patients. Our results indicated that HIF1A-AS2 functions as an oncogenic factor in adenocarcinoma cells by targeting the miR-146b-5p/IL-6/STAT3 axis and may be a prognostic indicator of survival. Moreover, it can be a potential therapeutic target to enhance the efficacy of osimertinib in LUAD patients.

INTRODUCTION

Lung cancer is the most frequently diagnosed malignant tumor and the leading cause of cancer-associated mortality worldwide.[1] Lung adenocarcinoma (LUAD) is the main histological type of lung cancer. Although great progress has been made in lung cancer diagnosis and systemic therapy, the overall 5-year survival rate remains lower than 20%.[2] Over the last few years, the third epidermal growth factor receptor (EGFR) tyrosine kinase inhibitor (TKI) osimertinib has significantly improved the prognosis of patients with LAUD.[3] However, the development of acquired resistance has limited treatment outcomes. Therefore, a better understanding of the underlying mechanism of osimertinib resistance is required to develop effective therapeutic strategies for patients with LAUD.

Long non-coding RNAs (lncRNAs), whose transcript lengths are over 200 nucleotides, are a cluster of nonprotein-coding RNAs.[4] Numerous studies have reported that lncRNAs play crucial regulatory roles in tumorigenesis, metastasis, and drug resistance by functioning as competing endogenous RNAs (ceRNAs), which could sponge microRNAs (miRNAs) and disrupt miRNA-mediated degradation of target mRNAs in several cancer types.[5–7] For example, lncRNA CCAT1 could upregulate HOXA1 expression by competitively binding to miR-218 to increase gefitinib resistance in non-small cell lung cancer (NSCLC).[8] The lncRNA UCA1 acts as a miR-143 sponge to promote gefitinib resistance in NSCLC by targeting FOSL2.[9] Furthermore, lncRNA HIF1A-AS2 has been involved in many human tissues and is associated with poor outcomes in various tumors, including bladder,[10] colorectal,[11] and breast cancer.[12,13] HIF1A-AS2 facilitates osteogenic differentiation of adipose-derived stem cells through the miR-665/IL-6 axis via the PI3K/Akt signaling pathway.[14] Importantly, the correlation between HIF1A-AS2 and chemoresistance has been identified. For example, the upregulated expression of HIF1A-AS2 hampers the p53 family protein-dependent apoptotic pathway to promote cisplatin resistance in bladder cancer.[15] Nevertheless, the molecular regulation mechanism of HIF1A-AS2 in carcinogenesis and osimertinib resistance in lung cancer has not been studied yet.

In this study, we found that HIF1A-AS2 was specifically upregulated in LUAD tissues. High expression of HIF1A-AS2 was significantly associated with poor overall and disease-free survival (DFS) in patients with LUAD. Gain- and loss-of-function assays revealed that

Received 14 February 2021; accepted 8 September 2021;
https://doi.org/10.1016/j.omtn.2021.09.003.

[3]These authors contributed equally

Correspondence: Hongyu Tan, MD, Department of Anesthesiology, Key Laboratory of Carcinogenesis and Translational Research (Ministry of Education), Peking University Cancer Hospital and Institute, Beijing 100142, China.
E-mail: maggitan@yeah.net
Correspondence: Yue Yang, MD, Department of Thoracic Surgery II, Key Laboratory of Carcinogenesis and Translational Research (Ministry of Education), Peking University Cancer Hospital and Institute, Beijing 100142, China.
E-mail: zlyangyue@bjmu.edu.cn

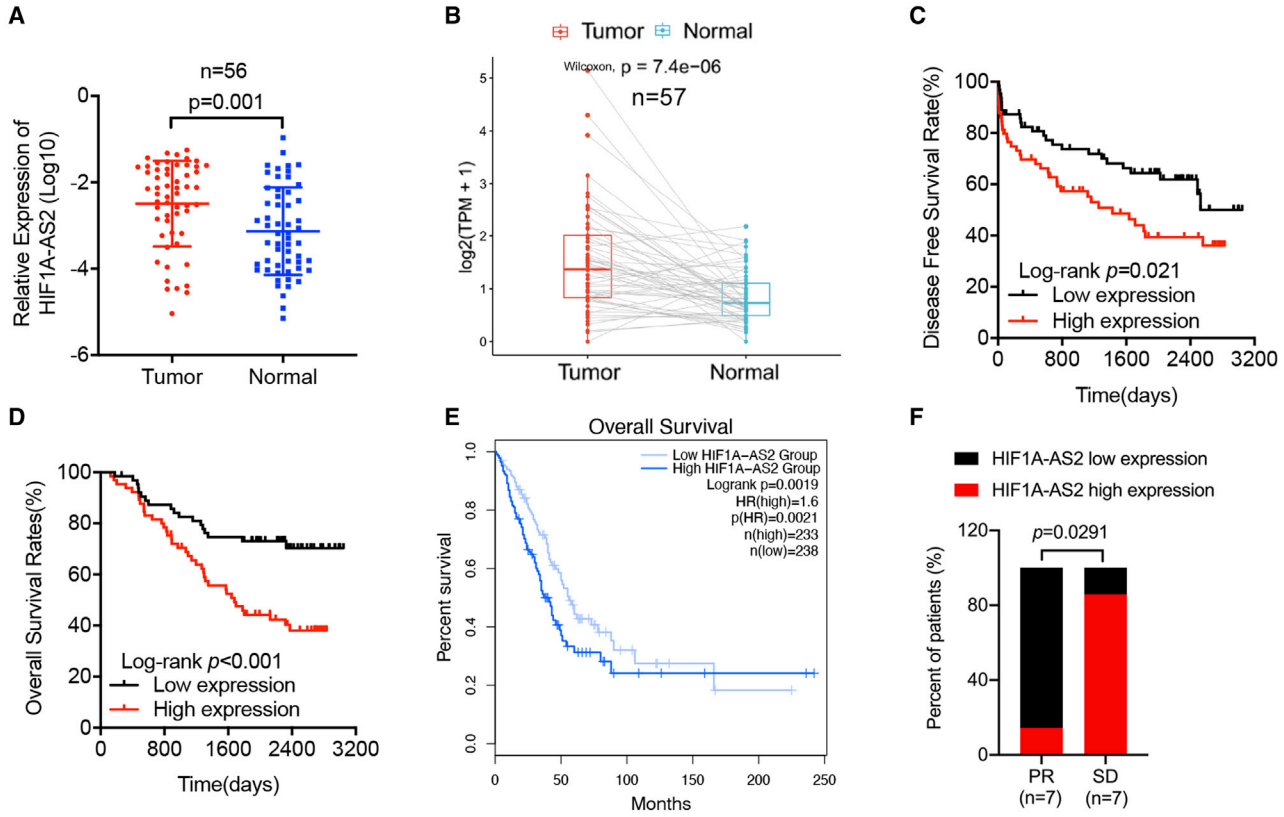

Figure 1. HIF1A-AS2 is upregulated in LUAD tissues and associated with a poor prognosis

(A) HIF1A-AS2 expression in 56 pairs of human LUAD tissues and adjacent non-tumor tissues was quantified by qRT-PCR. (B) TCGA database shows that HIF1A-AS2 expression was significantly upregulated in tumors compared with normal tissues. (C and D) Disease-free survival (C) and overall survival (OS) (D) of LUAD patients with relatively high and low expression of HIF1A-AS2, which were based on the median value of this lncRNA. (E) Kaplan-Meier analysis of OS for patients (TCGA). (F) The percentages of samples with high and low expression of HIF1A-AS2 in LUAD patients who received EGFR-TKI treatment (SD, n = 7; PR, n = 7) by qRT-PCR.

overexpression of HIF1A-AS2 promoted, whereas silencing HIF1A-AS2 attenuated the proliferation, migration, and tumorigenesis of LUAD cells and enhanced the susceptibility of tumor cells to osimertinib *in vitro* and *in vivo*, in which the miR-146b-5p/IL-6/STAT3 axis mediated the effects. Importantly, targeting HIF1A-AS2 not only inhibited the tumorigenesis of LUAD cells but also enhanced the therapeutic response of osimertinib-resistant LUAD cells to osimertinib *in vivo*.

RESULTS

HIF1A-AS2 was upregulated in LUAD tissues and associated with a poor prognosis

To investigate the role of HIF1A-AS2 in LUAD, we detected the relative expression of HIF1A-AS2 using qRT-PCR in 56 LUAD tissues and matched normal peritumoral tissues. As shown in Figure 1A, HIF1A-AS2 expression was markedly upregulated in LUAD tissues ($p < 0.05$). To validate the HIF1A-AS2 expression profile in LUAD, we investigated The Cancer Genome Atlas (TCGA)-LUAD database; HIF1A-AS2 expression was significantly upregulated in tumors compared with normal tissues (Figure 1B). Statistical analysis revealed no correlation between HIF1A-AS2 expression and the clinicopathological characteristics of 129 LUAD patients (Table S1). The DFS rates and overall survival (OS) rates of patients with high HIF1A-AS2 expression were significantly lower than those with low expression (Figures 1C and 1D). Furthermore, a Cox proportional hazards model was applied to analyze the effects of HIF1A-AS2 expression on OS and DFS. HIF1A-AS2 remained significantly associated with OS (Table S2) and DFS (Table S3). In the TCGA-LUAD database, OS was significantly greater in patients with low HIF1A-AS2 levels than in patients with high HIF1A-AS2 levels (Figure 1E). HIF1A-AS2 expression analysis in blood samples from advanced LUAD patients who received EGFR-TKI treatment showed that those with low HIF1A-AS2 expression had a good response (partial response, PR) to EGFR-TKI, whereas patients with high HIF1A-AS2 expression exhibited a poor response (stable disease, SD; Figure 1F).

These results suggested that the expression of long non-coding HIF1A-AS2 was remarkably elevated, which is related to a poor prognosis and osimertinib resistance in LUAD patients.

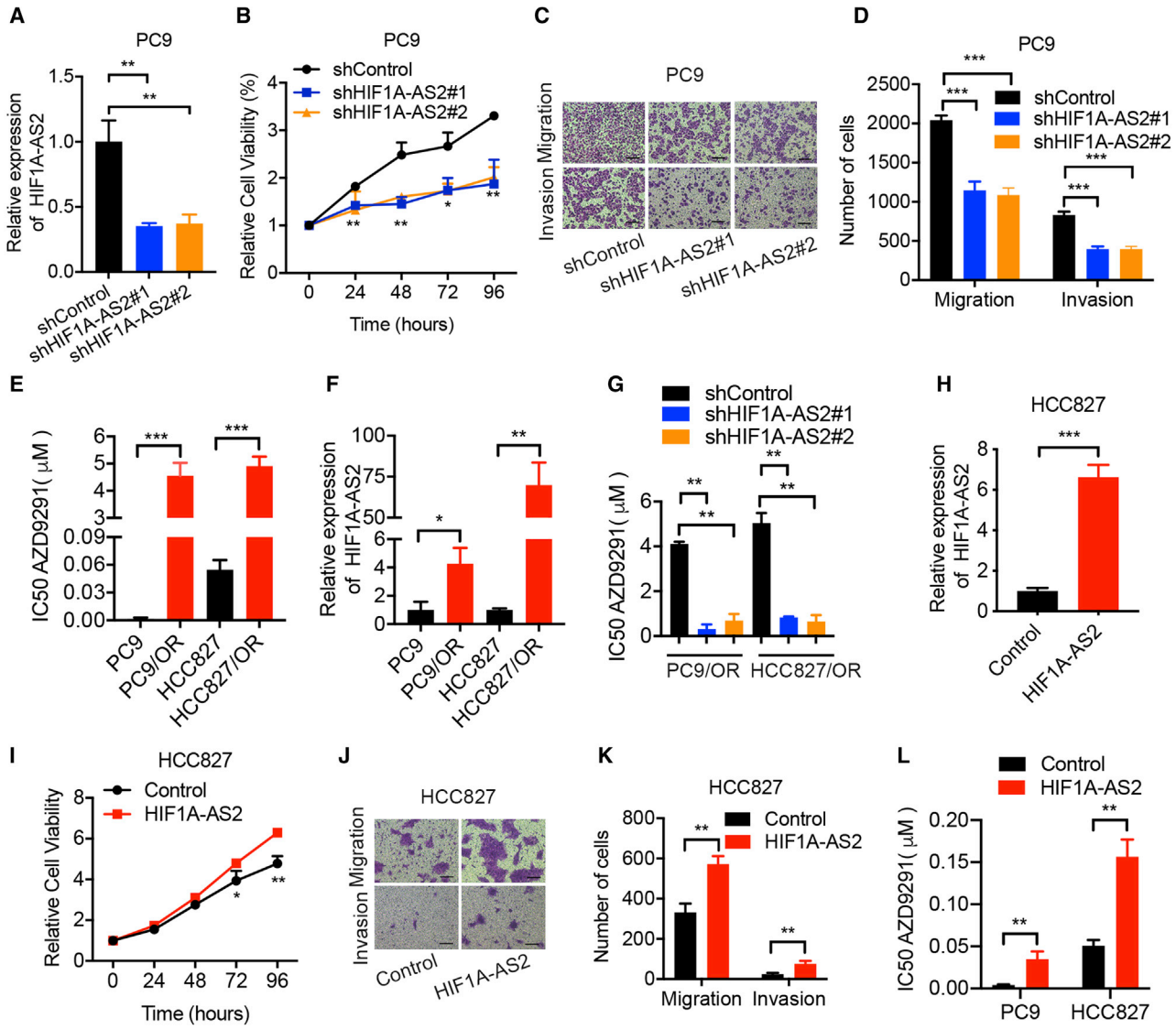

Figure 2. HIF1A-AS2 promoted LUAD cell proliferation, migration, invasion, and osimertinib resistance

(A) The HIF1A-AS2 expression in PC9 cells transfected with shHIF1A-AS2#1 and #2 via qRT-PCR. (B) Proliferation rate was detected in HIF1A-AS2 silencing PC9 cells, as indicated by the CCK-8 assay. (C and D) Knockdown of HIF1A-AS2 successfully reduced the migration and invasion ability of PC9 cells, as indicated by the transwell assay. Scale bar, 100 μm. (E) The histograms show the IC_{50} of osimertinib in PC9/OR, HCC827/OR, PC9, and HCC827. (F) The expression levels of HIF1A-AS2 were analyzed in PC9, PC9/OR, HCC827, and HCC827/OR cells by qRT-PCR. (G) IC_{50} values of osimertinib in the HIF1A-AS2-depleted PC9/OR and HCC827/OR cells. (H) The HIF1A-AS2 expression in HCC827 cells with HIF1A-AS2 overexpression by pReceiver vector via qRT-PCR. (I) Overexpression of HIF1A-AS2 increased HCC827 cell proliferation rate, as indicated by the CCK-8 assay. (J and K) upregulation of HIF1A-AS2 enhanced the migration and invasion ability of HCC827 cells, as indicated by the transwell assay. Scale bar, 100 μm. (L) IC_{50} values of osimertinib in PC9 and HCC827 cells with HIF1A-AS2 overexpression on by CCK-8 assay. *$p < 0.05$; **$p < 0.01$; ***$p < 0.001$.

HIF1A-AS2 knockdown inhibits proliferation, metastasis, and osimertinib resistance in LAUD cells

Compared with the human bronchial epithelial (HBE) cell line, HIF1A-AS2 expression was increased in PC9, A549, HCC827, and H1975 cells (Figure S1A). To explore the potential biological function of HIF1A-AS2 in LUAD, we transfected PC9 cells with short hairpin RNAs (shRNAs) targeting HIF1A-AS2 or a control shRNA. Transfection efficiency was confirmed using qRT-PCR at 48 h post-transfection (Figure 2A). HIF1A-AS2 knockdown decreased PC9 cell proliferation and the number of migrated and invasive cells (Figures 2B–2D).

Furthermore, we generated osimertinib-resistant PC9/OR and HCC827/OR cells derived from parental PC9 and HCC827 cells, which showed significantly increased inhibitory concentration (IC_{50}; Figure 2E). The relative expression of HIF1A-AS2 was higher in PC9/OR and HCC827/OR cells than in parental cells (Figure 2F).

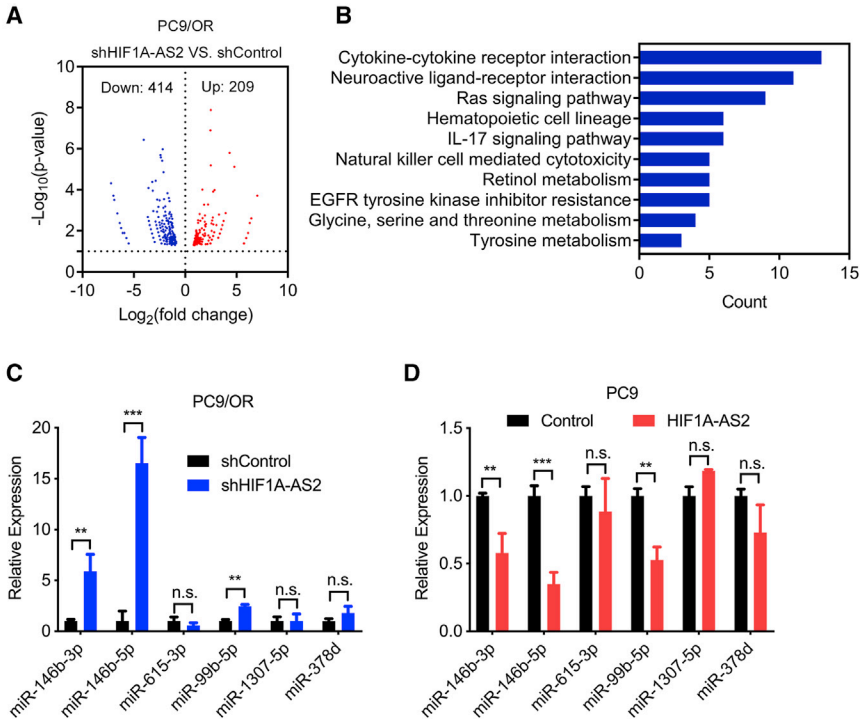

Figure 3. Negative correlation between HIF1A-AS2 and miR-146b-5p

(A) Volcano plot depicting a log transformation plot of the fold difference (x axis) and the p value (y axis) of indicated genes between PC9/OR-shHIF1A-AS2 and PC9/OR-shControl cells. (B) Signaling pathways were enriched in the PC9/OR-shHIF1A-AS2 cells over the control cells by Kyoto Encyclopedia of Genes and Genomes (KEGG) analysis. (C) miR-146b-3p, miR-146b-5p, miR-615-3p, miR-99b-5p, miR-1307-5p, and miR-378d expression was detected in PC9/OR cells with HIF1A-AS2 knockdown by qRT-PCR. (D) miR-146b-3p, miR-146b-5p, miR-615-3p, miR-99b-5p, miR-1307-5p, and miR-378d expression was tested in PC9 cells with HIF1A-AS2 overexpression by qRT-PCR.

Therefore, we determined whether HIF1A-AS2 influenced the sensitivity of LAUD cells to osimertinib. HIF1A-AS2-depleted PC9/OR, HCC827/OR, and control cells were established. Transfection efficiency was verified using qRT-PCR at 48 h post-transfection (Figure S1B). As shown in Figure 2G, compared with the control cells, the IC_{50} for osimertinib was significantly decreased in HIF1A-AS2-depleted PC9/OR and HCC827/OR cells.

These data suggest that HIF1A-AS2 knockdown inhibited proliferation, metastasis, and osimertinib resistance in LAUD cells.

Upregulation of HIF1A-AS2 promotes proliferation, metastasis, and osimertinib resistance in LAUD cells

We further investigated the function of HIF1A-AS2 by overexpression of HIF1A-AS2 in PC9 and HCC827 cells. We established stable HIF1A-AS2-overexpressed HCC287 cells through the transfection of the pReceiver- HIF1A-AS2 expression plasmid and the control cells (Figure 2H). Overexpression of HIF1A-AS2 promoted the proliferation, migration, and invasion abilities of HCC287 cells compared to control cells (Figures 2I–2K). In addition, we examined the influence of HIF1A-AS2 upregulation on the sensitivity of LAUD cells to osimertinib. Stable HIF1A-AS2-overexpressed PC9 cells and control cells were established. Transfection efficiency was verified using qRT-PCR at 48 h post-transfection (Figure S1C). As shown in Figure 2L, the upregulation of HIF1A-AS2 expression led to an increase in the IC_{50} for osimertinib in PC9 and HCC827 cells. These results indicated that HIF1A-AS2 promotes proliferation, metastasis, and osimertinib resistance in LAUD cells.

HIF1A-AS2 acts as a sponge for miR-146b-5p/IL-6 in LAUD

We performed RNA sequencing (RNA-seq) to explore potential target binding miRNAs and mRNAs of HIF1A-AS2 in PC9/OR cells with HIF1A-AS2 knockdown (Table S4). There were 209 upregulated genes and 414 downregulated genes (Figure 3A). Signaling pathways, including the cytokine-cytokine receptor interaction, IL-17 signaling pathway, and EGFR-TKI resistance, were altered when HIF1A-AS2 was suppressed (Figure 3B). Among potential candidate miRNAs, the expression levels of six miRNAs, including miR-146b-3p, miR-146b-5p, miR-615-3p, miR-99b-5p, miR-1307-5p, and miR-378d, were negatively correlated with HIF1A-AS2. qRT-PCR analysis confirmed that the expression of miR146b-3p, miR146b-5p, and miR99b-5p was substantially downregulated by the upregulation of HIF1A-AS2. In contrast, the silencing of HIF1A-AS2 enhanced the expression of miR146b-3p, miR146b-5p, and miR99b-5p (Figures 3C and 3D).

HIF1A-AS2 promotes LAUD malignant properties and osimertinib resistance by competing for miR-146b-5p

Bioinformatic analysis revealed putative complementary sequences between HIF1A-AS2 and miR146b-5p. To identify whether HIF1A-AS2 was indeed targeted by the miR146b-5p, wild-type (HIF1A-AS2-WT), and miR146b-5p binding site, we synthesized mutant type HIF1A-AS2 (HIF1A-AS2-Mut) luciferase reporters (Figure 4A). The results showed that co-transfection of HIF1A-AS2-WT with miR146b-5p mimics, but not HIF1A-AS2-Mut, remarkably reduced the luciferase activity in PC9 cells (Figure 4B). Moreover, we performed an RNA immunoprecipitation (RIP) assay to show that HIF1A-AS2 and miR146b-5p were preferentially enriched in Ago2-containing beads in LUAD cells, thus verifying the interaction between HIF1A-AS2 and miR146b-5p (Figure 4C).

As expected, compared with the control cells, treatment with anti-miR146b-5p increased cell proliferation and the number of migrated cells in PC9 cells (Figures S2A and S2B). In contrast, treatment with

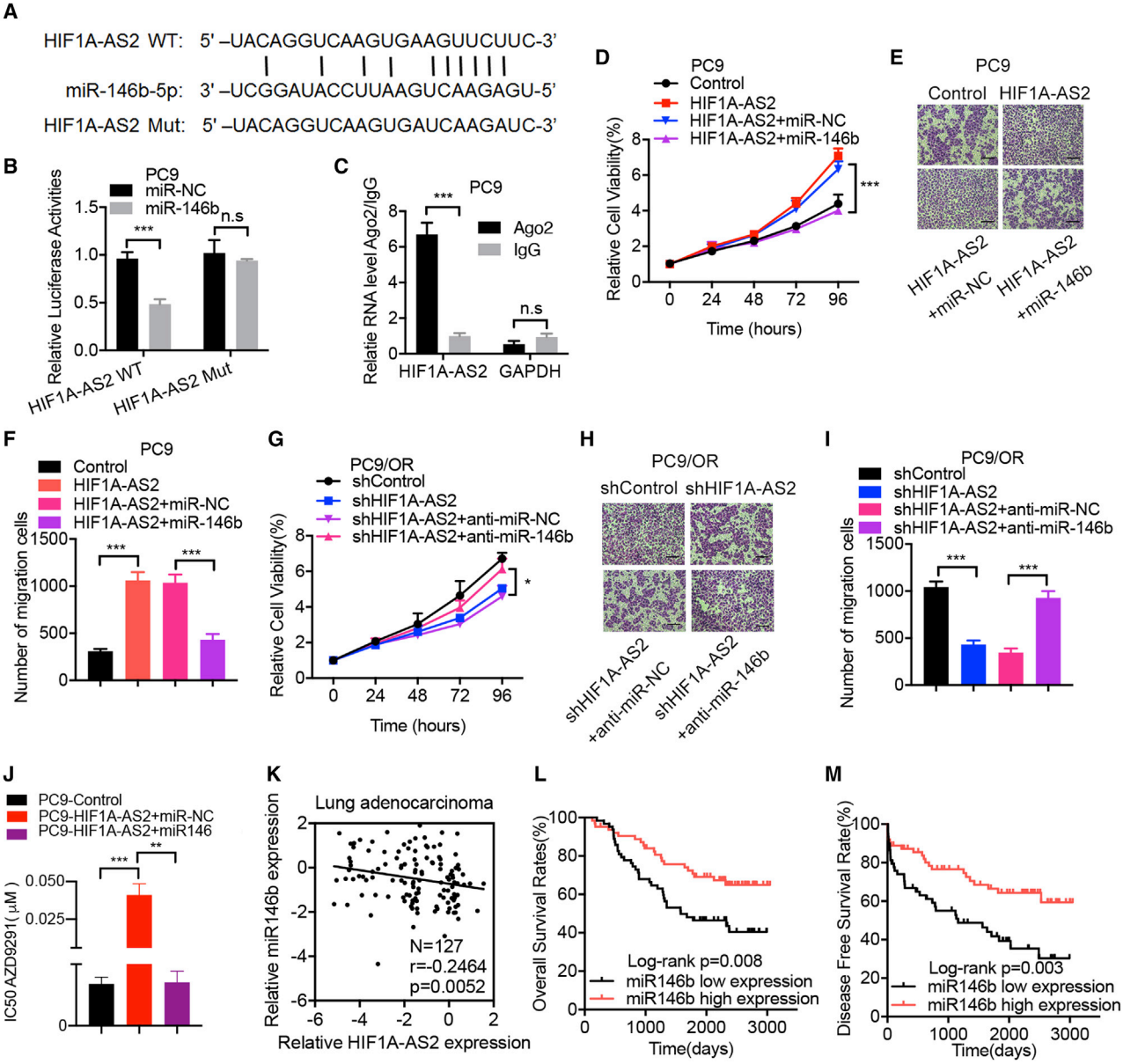

Figure 4. HIF1A-AS2 functions as a ceRNA for miR-146b-5p

(A) Potential binding sites of HIF1A-AS2 with miR-146b-5p (miR-146b), and wild-type (WT) and mutant (Mut) sequence of HIF1A-AS2 within the binding sites. (B) Luciferase activity of HIF1A-AS2-WT or HIF1A-AS2-Mut was evaluated by luciferase reporter assay with the transfection of miR-146b mimics. (C) RIP assay confirmed the interaction of miR-146b with HIF1A-AS2 in PC9 cells. (D) CCK-8 assay was used to assess cell viability of each group as indicated. (E and F) Cell migration was confirmed in each group by transwell assay. Scale bar, 100 μm. (G) CCK-8 assay was used to assess cell viability of each group. (H and I) Cell migration was confirmed in each group by transwell assay. Scale bar, 100 μm. (J) IC_{50} values of osimertinib was tested in each group by CCK-8 assay. (K) Spearman's correlation analysis confirmed the negative association between HIF1A-AS2 and miR-146b-5p. (L and M) Kaplan-Meier analysis and log-rank test identified the prognostic significance of miR-146b-5p in LUAD patients. Based on the median value of miR-146b-5p, the patients were divided into high and low expression groups. n.s., $p > 0.05$; *$p < 0.05$; **$p < 0.01$; ***$p < 0.001$.

miR146b-5p mimics decreased cell proliferation and the number of migrated cells in PC9/OR cells (Figures S2C and S2D). In addition, the relative expression of miR146b-5p was higher in PC9/OR cells than in PC9 cells (Figure S2E). Compared with the control cells, treatment with miR146b-5p inhibitor led to an increase in IC_{50} for osimertinib in PC9 cells (Figure S2F), whereas treatment with miR146b-5p mimics decreased the IC_{50} in PC9/OR cells (Figure S2G).

To verify the role of miR146b-5p in HIF1A-AS2 regulation of LUAD progression, we performed rescue experiments. The results revealed

that treatment with miR146b-5p mimics abolished cell proliferation and migration induced by HIF1A-AS2 overexpression in PC9 cells (Figures 4D–4F). In contrast, anti-miR146b-5p treatment weakened the inhibitory effects of HIF1A-AS2 downregulation on the proliferation and migration of PC9/OR cells (Figures 4G–4I). Moreover, the increased IC_{50} for osimertinib in PC9 cells with HIF1A-AS2 upregulation could be partially reversed by miR146b-5p mimics (Figure 4J).

To examine the clinical relevance of miR-146b-5p in LUAD, we measured miR-146b-5p expression using qRT-PCR in 127 samples of primary LUAD tissues. An inverse correlation between HIF1A-AS2 and miR-146b-5p expression was observed (Figure 4K). Patients with high miR-146b-5p expression had a favorable prognosis than those with low miR-146b-5p expression (Figures 4L and 4M). Moreover, lower expression of miR-146b-5p was detected in tumor tissues than in normal tissues in the TCGA-LUAD database (Figure S3A). There was no significant difference in the OS analysis between high and low miR-146b-5p expression in LUAD (Figure S3B, TCGA database).

These results show that HIF1A-AS2 functioned as ceRNA by sponging miR146b-5p, which could partially overcome the promoting effect of HIF1A-AS2 on the proliferation, migration, and osimertinib sensitivity of LUAD cells.

HIF1A-AS2 promotes LAUD malignant properties and osimertinib resistance by interfering with the miR-146b-5p/IL-6/STAT3 axis

Bioinformatics analysis predicted that IL-6 was the target gene of the HIF1A-AS2/miR-146b-5p axis. The potential binding sites between miR-146b-5p and the 3′ UTR regions of IL-6 were identified using bioinformatics tools (Figure 5A). Luciferase reporter assays showed that luciferase activity was lower in the IL-6-WT than in the IL-6-Mut vector (Figure 5B). To clarify the relationship between HIF1A-AS2 and IL-6, we performed qRT-PCR to determine the expression of IL-6 in LAUD cells with HIF1A-AS2 overexpression or knockdown. The results showed that upregulation of HIF1A-AS2 enhanced the expression of IL-6 in PC9 cells (Figure 5C), whereas silencing HIF1A-AS2 inhibited IL-6 expression in PC9/OR cells (Figure 5D), as validated using western blotting (Figure 5E). We hypothesized that HIF1A-AS2 might function by interacting with miR146b-5p, thereby activating the IL-6/STAT3 pathway. Next, we explored the association between the HIF1A-AS2 and STAT3 pathways. Western blotting verified an increase in the protein levels of p-STAT3 in PC9 cells with HIF1A-AS2 overexpression but a decrease in PC9/OR cells with HIF1A-AS2 knockdown. Notably, STAT3 levels remained constant (Figure 5E; Figure S4A). Moreover, IL-6 and p-STAT3 upregulation induced by HIF1A-AS2 overexpression was abrogated by miR-146b-5p mimics in PC9 cells (Figure 5F; Figure S4B). Consistently, shHIF1A-AS2 downregulated IL-6 and p-STAT3 expression, which was substantially abolished by the miR-146b-5p inhibitor in PC9/OR cells (Figure 5G; Figure S4C).

We next determined IL-6 and STAT3 expression in osimertinib-resistant PC9/OR and parental PC9 cells and explored their effect on the sensitivity of LAUD cells to osimertinib. As shown in Figure S4D, IL-6 and STAT3 exhibited higher expression in PC9/OR cells than in PC9 cells. Compared with the control cells, the knockdown of IL-6 expression or treatment with cryptotanshinone (STAT3 inhibitor) led to a decrease in the IC_{50} for osimertinib in PC9/OR cells (Figures S4E and S4F). In PC9 cells with overexpressed HIF1A-AS2, the increased IC_{50} of osimertinib could be partially reversed by the downregulated expression of IL-6 or cryptotanshinone treatment (Figures 5H and 5I).

Next, we analyzed HIF1A-AS2, IL-6, and miR146b-5p expression in the LUAD samples (n = 127), which exhibited a positive correlation between HIF1A-AS2 and IL-6 and a negative correlation between IL-6 and miR146b-5p (Figure 5J; Figure S4G). Moreover, high IL-6 expression suggested low DFS and OS in patients with LUAD (Figures 5K and 5M).

Overall, the above data indicated that HIF1A-AS2 might activate the IL-6/STAT3 pathway by binding to miR146b-5p to promote LUAD malignant features.

Targeting HIF1A-AS2 inhibits tumor growth and osimertinib resistance *in vivo*

To explore the role of HIF1A-AS2 in tumorigenesis *in vivo*, we performed a xenograft tumor assay. PC9-HIF1A-AS2, PC9-Control, PC9/OR-shHIF1A-AS2, and PC9/OR-shControl cells were injected into the right dorsal flank of female BALB/c nude mice, and tumor growth was quantified. Compared with the control groups, upregulating HIF1A-AS2 remarkably enhanced tumor volume and weight. In contrast, silencing HIF1A-AS2 reduced tumor volume and weight (Figures 6A–6C).

HIF1A-AS2 expression was upregulated in the tumor tissues acquired from mice implanted with PC9-HIF1A-AS2 cells compared with those from mice inoculated with the control cells. In contrast, HIF1A-AS2 expression was reduced in the tumor tissues from the mice inoculated with PC9/OR-shHIF1A-AS2 cells (Figure 6D). The expression of miR-146b-5p was reduced in tumor tissues from mice inoculated with PC9-HIF1A-AS2 cells compared to those from the mice inoculated with the control cells. In contrast, the miR-146b-5p expression was increased in tumor tissues from mice inoculated with PC9/OR-shHIF1A-AS2 cells (Figure 6E).

Next, we analyzed Ki-67, IL-6, and p-STAT3 expression using immunohistochemistry (IHC) in the tumor tissues. Conversely, Ki-67, IL-6, and p-STAT3 expression was significantly enhanced in tumors from PC9-HIF1A-AS2 mice compared to those from PC9-Control mice. In contrast, Ki-67, IL-6, and p-STAT3 expression decreased in tumors from PC9/OR-shHIF1A-AS2 mice compared with those from PC9/OR-shControl mice (Figure 6F; Figure S5A). The results demonstrated an inverse correlation between HIF1A-AS2 and miR-146b-5p and a positive relationship between HIF1A-AS2 and IL-6 and p-STAT3 expression in tumor tissues from mice inoculated with LUAD cells.

To explore the effect of *in vivo* HIF1A-AS2 targeted on tumor growth of LUAD cells resistant to osimertinib, we designed and

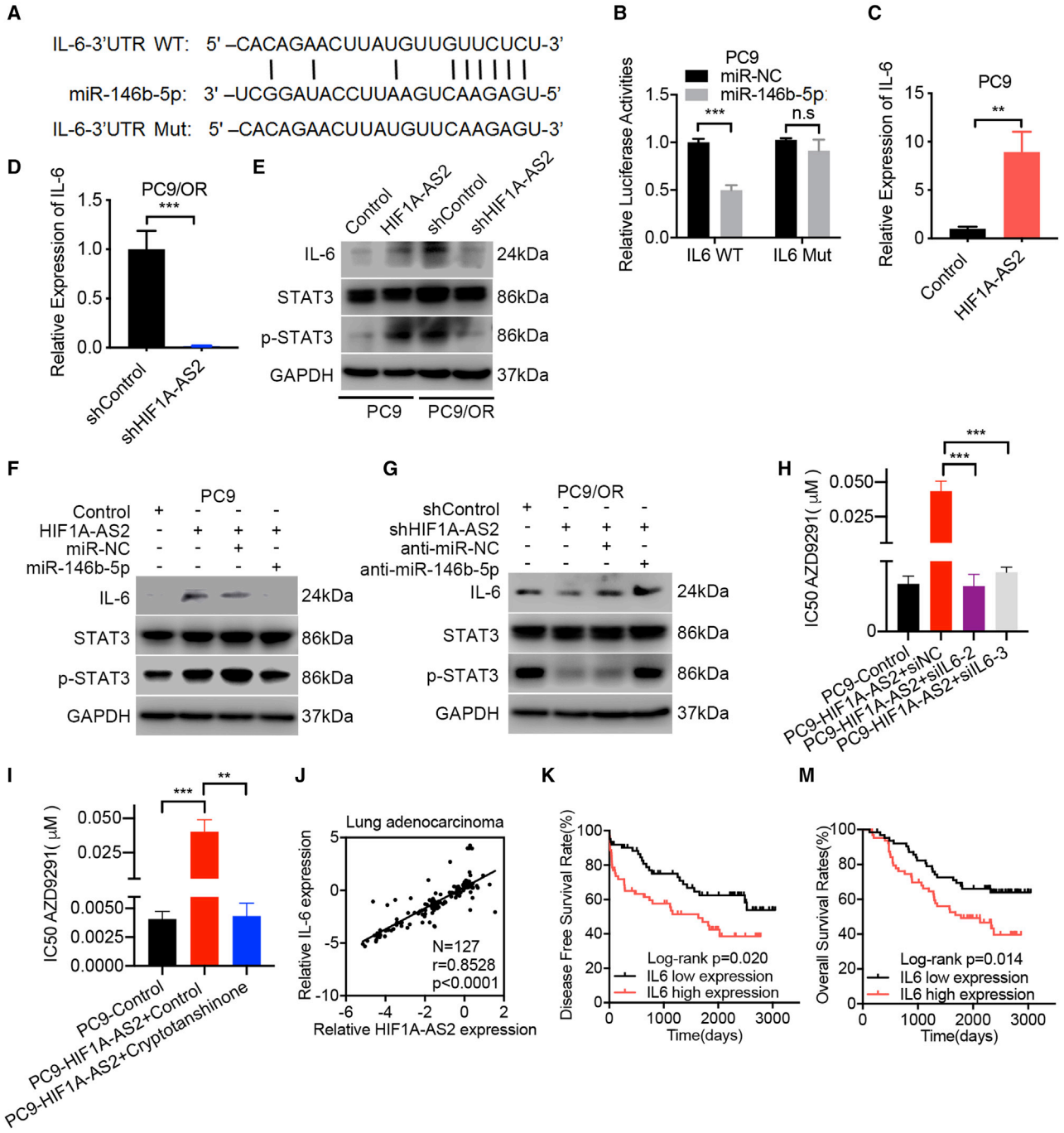

Figure 5. IL-6 was a target of HIF1A-AS2/miR-146b-5p in LUAD cells

(A) Potential binding sites of miR-146b-5p with 3′ UTR of IL-6, and the sequences of WT and Mut for the binding sites. (B) Luciferase activity of IL-6-WT or IL-6-Mut was evaluated by luciferase reporter assay with the transfection of miR-146b-5p mimics. (C) IL-6 expression was tested in PC9 cells with HIF1A-AS2 overexpression by qRT-PCR. (D) IL-6 expression was tested in PC9/OR cells with HIF1A-AS2 knockdown by qRT-PCR. (E) Western blot analysis of the IL-6, STAT3, and p-STAT3 expression in PC9/OR cells under HIF1A-AS2 downregulation, and in PC9 cells with upregulation of HIF1A-AS2. (F and G) Western blot results of IL-6, STAT3, and p-STAT3 expression in each group. GAPDH was used as a loading control. (H and I) IC_{50} values of osimertinib was analyzed in each group by CCK-8 assay. (J) Spearman's correlation analysis confirmed the positive association between HIF1A-AS2 and IL-6. (K and M) Kaplan-Meier analysis and log-rank test identified the prognostic significance of IL-6 in LUAD patients. Based on the median value of IL-6, the patients were divided into high and low expression groups. n.s., $p > 0.05$; **$p < 0.01$; ***$p < 0.001$.

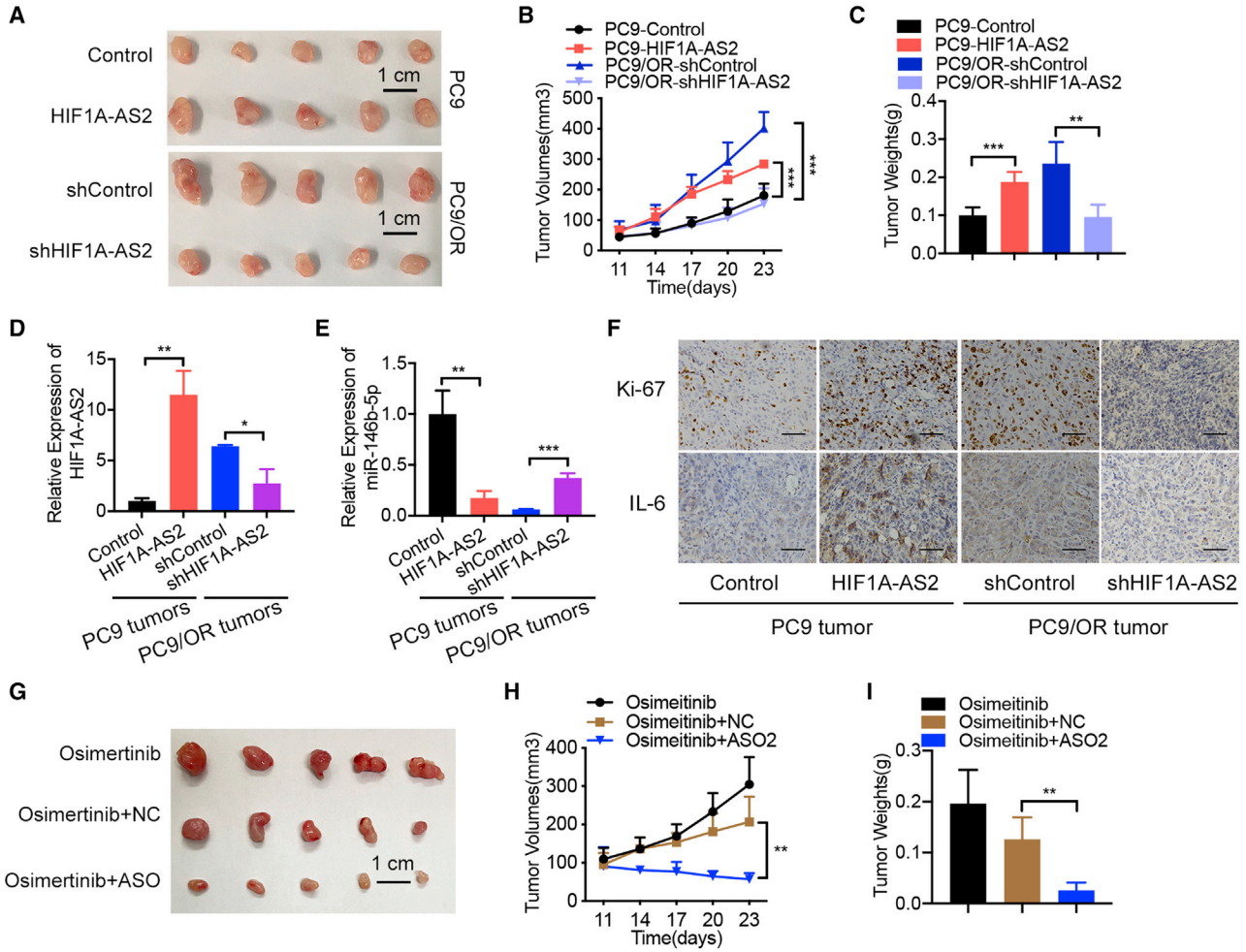

Figure 6. Targeting HIF1A-AS2 inhibited tumorigenesis and the susceptibilities of tumor cells to osimertinib *in vivo*

(A) Representative xenograft images of PC9-Control, PC9-HIF1A-AS2, PC9/OR-shControl, and PC9/OR-shHIF1A-AS2 tumors. (B) Growth curves in PC9-Control, PC9-HIF1A-AS2, PC9/OR-shControl, and PC9/OR-shHIF1A-AS2 models. (C) Histogram of tumor weights in PC9-Control, PC9-HIF1A-AS2, PC9/OR-shControl, and PC9/OR-shHIF1A-AS2 tumors. (D and E) qRT-PCR analysis identified the expression of HIF1A-AS2 (D) and miR-146b-5p (E) in the indicated tumor tissues. (F) Representative images (×200 magnification) of Ki-67 and IL-6 staining by immunohistochemical analysis in tumor tissues. Scale bars, 50 μm. (G) Representative xenograft images of PC9/OR tumors with osimertinib (25 mg/kg/d), osimertinib (25 mg/kg/d) plus NC (5 nmol), and osimertinib (25 mg/kg/d) plus ASO (5 nmol). (H) Growth curves in PC9/OR models with osimertinib, Osimertinib+NC, or Osimertinib+ASO treatment at the indicated time points. (I) Histogram of tumor weights in PC9/OR models with the indicated treatments. Data are presented as the means ± SDs; n = 5. **p < 0.01; ***p < 0.001.

used an ASO targeting HIF1A-AS2 as an antagonist to inhibit endogenous HIF1A-AS2 expression. HIF1A-AS2 was inhibited in PC9/OR cells treated with ASO (Figure S5B). Based on our previous study,[16] we injected PC9/OR cells resistant to osimertinib into the right dorsal flank of female BALB/c nude mice. When the tumor volume reached 100 mm^3, the mice were randomly divided into three groups (n = 5 per group) and treated with osimertinib (25 mg/kg/do) via oral gavage, osimertinib plus lncRNA ASO negative control (NC), or osimertinib plus ASO-h-HIF1A-AS2 (ASO) by intratumor injection. No significant change in tumor growth was detected between the osimertinib and osimertinib plus NC groups. Importantly, the combination of osimertinib and ASO treatment dramatically suppressed tumor growth, with a tumor growth inhibition rate of 72.4%, compared with the osimertinib plus NC group (Figures 6G and 6H). The tumor weights were also significantly suppressed in the combined treatment with osimertinib plus ASO compared with the NC group (Figure 6I). In addition, osimertinib plus ASO resulted in the inhibition of HIF1A-AS2 expression (Figure S5C).

Collectively, these results suggested that HIF1A-AS2 inhibition could represent a valid therapeutic strategy for LUAD patients resistant to osimertinib, which is regulated by the miR-146b-5p/IL-6/STAT3 axis (Figure 7)

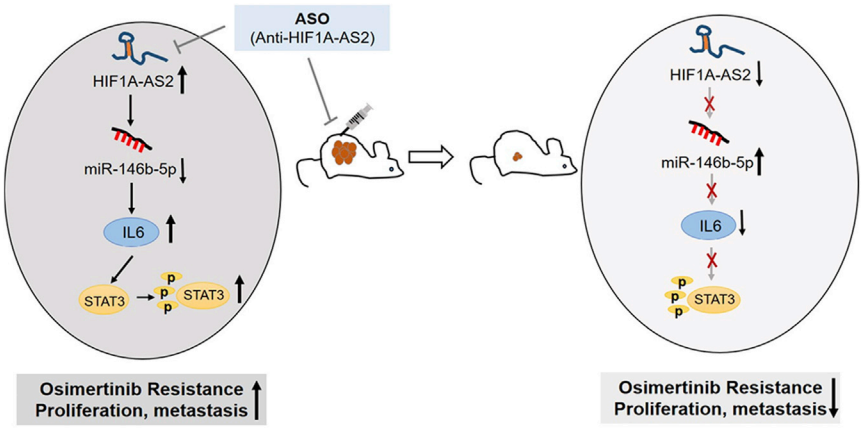

Figure 7. A schematic diagram shows HIF1A-AS2 mediated miR-146b-5p/IL6/STAT3 regulation in proliferation, metastasis, and osimertinib resistance and that targeting this axis overcomes the malignant properties of LUAD

DISCUSSION

The primary results of this study provide novel insights into the significant role of HIF1A-AS2 in the tumorigenesis and osimertinib resistance of LUAD cells via the miR-146b-5p /IL-6/STAT3 axis. We identified that lncRNA HIF1A-AS2 acts as an oncogene in LUAD and reported that HIF1A-AS2 is enhanced in clinical LUAD tissues and is associated with survival in LUAD patients. Our results further revealed that HIF1A-AS2 promoted the proliferation, migration, tumorigenesis, and osimertinib resistance of LUAD cells by disrupting the repressive effect of miR-146b-5p on IL-6 expression by sponging miR-146b-5p. Importantly, targeting HIF1A-AS2 by ASO reinforced the therapeutic sensitivity of osimertinib-resistant cells to osimertinib *in vivo*. Therefore, our results revealed a novel mechanism by which HIF1A-AS2 promoted the proliferation, migration, and tumorigenesis of LUAD cells and inhibited the susceptibility of tumor cells to osimertinib, indicating that HIF1A-AS2 could be a potential therapeutic target to enhance the efficacy of osimertinib in LUAD.

Previous studies have revealed that HIF1A-AS2 is a type of lncRNA that promote cancer progression, and its role has been reported in many cancer studies, such as osteosarcoma,[17] ovarian,[18] and gastric cancer.[19] Consistently, HIF1A-AS2 contributed to proliferation, metastasis, and tumorigenesis of LUAD cells, indicating that HIF1A-AS2 is a positive regulator in the development of LUAD. It has been reported that there is an association of high HIF1A-AS2 expression with shorter OS in triple-negative breast cancer,[13] gastric cancer,[20] and bladder cancer.[10] In the clinical samples, HIF1A-AS2 was upregulated in LUAD tissues and was associated with an unfavorable prognosis in LUAD patients.

HIF1A-AS2 has been implicated in chemoresistance, such as cisplatin resistance in bladder cancer,[15] but it has not been associated with drug resistance in LUAD. In the clinical blood specimens, high expression of this lncRNA related to poor response to EGFR-TKI treatment. Additionally, silencing HIF1A-AS2 enhanced the therapeutic sensitivity of osimertinib-resistant LUAD cells to osimertinib *in vivo*. Collectively, we demonstrated that HIF1A-AS2 exhibited oncogenic properties in LUAD, as well as the potential therapeutic efficacy of HIF1A-AS2 as a sensitizer of EGFR-TKI resistance in LUAD.

Recent studies have shown that lncRNAs function to relieve miRNA-mediated target mRNA degradation as ceRNAs.[21,22] In this study, we revealed that miR-146b-5p was negatively associated with HIF1A-AS2, indicating that HIF1A-AS2 can function as a sponge in osimertinib-resistant LUAD. Although numerous studies have investigated the role of miR-146b-5p in human malignancies, its role in tumor progression remains controversial. Zhu et al.[23] reported that miR-146b-5p could function as an oncogene in colorectal cancer. miR-146b-5p has been identified as an miRNA suppressor and prognosis predictor in NSCLC.[24] Accumulating evidence suggests that lncRNAs may be involved in developing cancers by interacting with miR-146b-5p.[25,26] In our results, the interaction between miR-146b-5p and HIF1A-AS2 was verified. Upregulation of miR-146b-5p has been shown to inhibit cell proliferation and migration and enhance the drug sensitivity of LUAD cells to osimertinib. Moreover, HIF1A-AS2 was negatively correlated with miR-146b-5p, and miR-146b-5p mediated the role of HIF1A-AS2 in LUAD.

In the current study, IL-6 was the direct target of the HIF1A-AS2/miR-146b-5p axis. The positive relationship between IL-6 and HIF1A-AS2 and the negative association between IL-6 and miR-146b-5p were identified in LUAD. High expression of IL-6 in tumor tissue is related to lung cancer progression, therapy resistance, and unfavorable prognosis in patients with lung cancer.[27,28] Moreover, previous studies have revealed that the IL-6/STAT3 signaling pathway plays a crucial role in cell growth and survival.[29] STAT3 is activated through phosphorylation and is involved in lung cancer progression, resistance to antitumor therapies, and shorter survival of lung cancer patients.[30,31] In addition, our findings were consistent with other studies in that high IL-6 levels in tumor tissues were predictive of poor outcomes in LUAD patients, and miR-146b-5p mimics markedly abrogated the activation of the IL-6/STAT3 signaling pathway mediated by HIF1A-AS2 upregulation in LUAD cells. Collectively, our data revealed the underlying mechanism responsible for the role of HIF1A-AS2 through inhibiting miR-146b-5p following by activating IL-6/STAT3 in EGFR-TKI resistant LUAD.

Importantly, our results illustrated that targeting HIF1A-AS2 reduced the tumor growth of LUAD cells and significantly enhanced the susceptibility of osimertinib-resistant cells to osimertinib *in vivo*, identifying the potential therapeutic efficacy of HIF1A-AS2 as a targeted therapy sensitizer in LUAD. This may explain that HIF1A-AS2 was highly

expressed in LUAD tissues and osimertinib-resistant cells and was associated with cell proliferation, migration, and osimertinib resistance in LUAD. Moreover, HIF1A-AS2 activated the STAT3 signaling pathway by upregulating IL-6 expression by sponging miR-146b-5p as a ceRNA, which induced osimertinib resistance and tumor growth *in vivo*. Therefore, our results provide experimental evidence that HIF1A-AS2 is a potential therapeutic target in LUAD.

MATERIALS AND METHODS

Re-analyses of TCGA LUAD database

We retrieved and reanalyzed original lncRNA and miRNA expression and clinical data from TCGA (http://cancergenome.nih.gov) database to investigate the clinical relevance of HIF1A-AS2 and miR-146b-5p with respect to the pathological traits of patients.

Patient and specimens

In total, 129 LUAD tissues and paired adjacent non-tumor tissues (n = 56) used in this study were obtained from patients during surgery at the Department of Thoracic Surgery, Peking University Cancer Hospital (Beijing, China) from January 2011 to November 2012. All fresh samples were snap-frozen immediately in liquid nitrogen and stored at −80°C until total RNA was extracted. Blood samples from 14 patients with EGFR Mut stage III-IV LUAD who received EGFR-TKI treatment (gefitinib, icotinib, afatinib, osimertinib, or dacomtinib) were enrolled from January 2017 to March 2021. Response to treatment was evaluated according to the Response Evaluation Criteria in Solid Tumors. Each case was diagnosed by histological staging according to the TNM classification. All patients received regular follow-ups, and clinical outcomes were determined. The study was approved by the Ethics Committee of Peking University Cancer Hospital, and written informed consent was obtained from all participants.

Cell line and culture

Human LUAD cell lines (PC9, A549, HCC827, and H1975) and HBE were maintained in our laboratory. The cell lines were cultured in RPMI 1640 medium (GIBCO BRL, Gaithersburg, MD, USA) containing 10% fetal bovine serum (FBS; GIBCO BRL) and 1% penicillin-streptomycin (P/S; Invitrogen, Grand Island, NY, USA) at 37°C in an atmosphere containing 5% CO_2. All cell lines were verified using short-tandem repeat (STR) analysis. Generation of EGFR-TKI-resistant cells (PC9/OR and HCC827/OR) was performed as described previously.[16]

Reagents

Osimertinib and cryptotanshinone (STAT3 inhibitor) were purchased from Selleck Chemicals (Houston, TX, USA). Reagents were formulated and stored according to the manufacturer's protocols.

RNA extraction and quantitative real-time PCR

Total RNA from clinical tissues and LUAD cells was extracted using TRIzol reagent (Invitrogen, Carlsbad, CA, USA) according to the manufacturer's instructions. cDNA was synthesized from total RNA (2 μg) using a commercially available kit (EasyScript First-Strand cDNA Synthesis SuperMix, Transgen Biotech, Beijing, China). Cellular RNA was purified from fresh whole blood using a QIAamp RNA Blood Mini Kit (52304, Hilden, Germany) according to the manufacturer's instructions. For detection of miR-146b-5p, cDNA was synthesized using the TaqMan MicroRNA Reverse Transcription Kit (Applied Biosystems, Foster City, CA, USA) according to the manufacturer's instructions. lncRNA, miRNA, and mRNA levels were assessed with the LightCycler 480 SYBR Green I Master using a LightCycler 480 Real-Time PCR System (Roche, Mannheim, Germany). GAPDH or small nuclear RNA U6 served as an internal control. The primers used are presented in Table S5.

Immunohistochemistry

Formalin-fixed and paraffin-embedded LUAD samples were incubated with primary anti-IL-6 (1:400 dilution; Proteintech Group, Rosemont, IL, USA) or Ki-67 (1:200 dilution; ZSGB-BIO, Beijing, China) overnight at 4°C followed by immunoglobulin G (IgG)/horseradish peroxidase (HRP) polymer (ZSGB-BIO) and diaminobenzidine substrate (ZSGB-BIO) in compliance with protocols. Two experienced pathologists independently evaluated the staining results.

Vector construction, oligonucleotides, and transfection

Shanghai GenePharma designed shRNA targeting HIF1A-AS2 and a NC. The pReceiver vector for HIF1A-AS2 overexpression and the NC was constructed by Genecopoiea. The hsa-miR-146b-5p mimic, hsa-miR-146b-5p inhibitor, and NC oligonucleotides were purchased from Ribobio (Guangzhou, China). Small interfering RNA (siRNA) targeting IL-6 and a NC were also purchased from Ribobio. The ASO-h-HIF1A-AS2 (ASO) and lncRNA ASO NCs were also purchased from Ribobio. The sequences are presented in Table S6. Transfection was performed using Lipofectamine 3000 (Invitrogen, Carlsbad, CA, USA) according to the manufacturer's instructions. After transduction, the cells were treated with 10 mg/mL neomycin to establish stable cell lines.

Luciferase reporter assay

The full-length sequence and fragment of HIF1A-AS2 that contained the indicated miRNA binding sequences were inserted into the pGL3-control vectors. The 3′ UTR fragments of IL-6 containing the binding sequence for specific miRNAs were also inserted into the pGL3-control vectors. PC9 cells were seeded in 96-well plates. At 48 h after co-transfection with miR-146b-5p mimics and the corresponding luciferase reporter vectors, luciferase activity was measured using the Dual-Luciferase Reporter Assay System (Promega, Madison, WI, USA).

Western blot assay

Total proteins were obtained from cells and quantified using a BCA Protein Assay Kit (Beyotime, Shanghai, China). Equal amounts of protein were separated using 10% SDS-PAGE and transferred to polyvinylidene fluoride (PVDF) membranes. After blocking with 5% BSA (Amresco) or fat-free milk at room temperature for 1 h, the membrane was probed with primary antibodies at a proper dilution at 4°C overnight, followed by secondary antibodies at room temperature for 1 h

and then visualized using chemiluminescence reagents. The primary antibodies included those against STAT3 (1:1,000, CST, Danvers, MA, USA), p-STAT3 (1:1,000, CST, Danvers), and IL-6 (1:1,000, Proteintech Group). GAPDH (1:1,000, CST, Danvers) was used as a control. Signals were visualized using an Amersham Imager 600 (GE Healthcare, Chicago, IL, USA) after incubation with Clarity Western ECL substrate (Bio-Rad, Hercules, CA). Protein expression was quantified using ImageJ software and normalized to GAPDH levels, followed by calculating ratios relative to controls.

Migration and invasion assays

In total, 1.0×10^5 cells per well in serum-free media were seeded into the upper chambers that were covered with (invasion) or without (migration; Matrigel, BD, USA). The lower chambers were filled with culture medium supplemented with 10% FBS. After 12 to 24 h, the cells that had migrated or invaded through the upper chamber were fixed in paraformaldehyde (4%) and stained with 0.1% crystal violet for 5 min at room temperature. An inverted microscope (Canon, Japan) was used to count and capture the images.

Cell viability

PC9, HCC827, and PC9/OR cells (1×10^3 cells/well) were seeded in 96-well plates. Cell counting kit-8 (CCK-8; Dojindo Molecular Technologies, Kumamoto, Japan) was used to monitor cell proliferation at 24, 48, 72, and 96 h, according to the manufacturer's protocol. The cell half-maximal IC_{50} was calculated using GraphPad software. The experiments were repeated three times.

RNA-binding protein immunoprecipitation assay

The Magna RIP kit (Millipore, USA) was used to perform the RIP assay. The PC9 cell lysate was incubated in RIP buffer containing magnetic beads and conjugated with human anti-Ago2 antibody; the input or normal rabbit IgG was included as a NC. Proteinase K was used to purify immunoprecipitated RNA. Quantitative real-time PCR was performed to detect the binding of target HIF1A-AS2 and miR-146b-5p.

Xenografts and treatments

Animal experiments were conducted to examine the role of HIF1A-AS2 *in vivo*, following the guidelines approved by the Ethics Committee of Animal Experiments of Peking University Cancer Hospital. In total, 2×10^6 cells were subcutaneously injected into 7-week-old female BALB/c nude mice (Beijing HFK Bioscience, China). Tumor volume was monitored and recorded every 4 days. Tumor volume was evaluated as follows: volume = length $\times$ width^2/2. After 28 days, the tumors were resected for further analysis.

In total, 2×10^6 PC9/OR cells were injected subcutaneously into the nude mice. When tumors reached approximately 100 mm^3, the mice were randomized into three groups (n = 5/group). The three groups were treated with osimertinib via oral gavage 5 days/week, osimertinib (5 days/week) plus 5 nmol ASO (synthesized in Ribobio) via intratumoral injection twice a week, or osimertinib (5 days/week) plus 5 nmol NC (synthesized in Ribobio) via intratumoral injection twice a week. Tumors were measured every 4 days using calipers. At the end of the treatments, the mice were sacrificed with CO_2, and the tumors were stripped for subsequent assays.

Statistical analysis

All experiments were conducted in triplicate. Data are expressed as the mean ± standard deviation (SD). OS was analyzed using Kaplan-Meier analysis and log-rank test. Spearman's correlation analysis was used to determine linear correlations between two variables. Two-group differences were examined using Student's t test, and multi-group differences were examined using a one-way ANOVA. Statistical significance was determined as $p < 0.05$.

SUPPLEMENTAL INFORMATION

Supplemental information can be found online at https://doi.org/10.1016/j.omtn.2021.09.003.

ACKNOWLEDGMENTS

This study was funded by the National Natural Science Foundation of China (grant number 81772494), Beijing Natural Science Foundation (grant number 7212009), Beijing Hospitals Authority' Ascent Plan (grant number DFL20191101), Wu Jieping Medical Foundation (grant number 213-16-276), and Science Foundation of Peking University Cancer Hospital (grant number 2020-2).

AUTHOR CONTRIBUTIONS

Y.Y. and H.T. designed and supervised the experiments. C.L. and Y.H. collected samples and collated the data. J.S. and Y.M. carried out the experiments and analyzed the data and contributed to drafting the manuscript. All authors reviewed and approved the final submitted manuscript.

DECLARATION OF INTERESTS

The authors declare no competing interests.

REFERENCES

1. Siegel, R.L., Miller, K.D., and Jemal, A. (2020). Cancer statistics, 2020. CA Cancer J. Clin. *70*, 7–30.
2. Martin, P., and Leighl, N.B. (2017). Review of the use of pretest probability for molecular testing in non-small cell lung cancer and overview of new mutations that may affect clinical practice. Ther. Adv. Med. Oncol. *9*, 405–414.
3. Gridelli, C., De Marinis, F., Di Maio, M., Cortinovis, D., Cappuzzo, F., and Mok, T. (2011). Gefitinib as first-line treatment for patients with advanced non-small-cell lung cancer with activating epidermal growth factor receptor mutation: Review of the evidence. Lung Cancer *71*, 249–257.
4. Chen, C., He, W., Huang, J., Wang, B., Li, H., Cai, Q., Su, F., Bi, J., Liu, H., Zhang, B., et al. (2018). LNMAT1 promotes lymphatic metastasis of bladder cancer via CCL2 dependent macrophage recruitment. Nat. Commun. *9*, 3826.
5. Karreth, F.A., Tay, Y., Perna, D., Ala, U., Tan, S.M., Rust, A.G., DeNicola, G., Webster, K.A., Weiss, D., Perez-Mancera, P.A., et al. (2011). In vivo identification of tumor- suppressive PTEN ceRNAs in an oncogenic BRAF-induced mouse model of melanoma. Cell *147*, 382–395.
6. Chen, J., Liu, A., Wang, Z., Wang, B., Chai, X., Lu, W., Cao, T., Li, R., Wu, M., Lu, Z., et al. (2020). LINC00173.v1 promotes angiogenesis and progression of lung squamous cell carcinoma by sponging miR-511-5p to regulate VEGFA expression. Mol. Cancer *19*, 98.

7. Huang, J., Pan, B., Xia, G., Zhu, J., Li, C., and Feng, J. (2020). LncRNA SNHG15 regulates EGFR-TKI acquired resistance in lung adenocarcinoma through sponging miR-451 to upregulate MDR-1. Cell Death Dis. *11*, 525.
8. Jin, X., Liu, X., Zhang, Z., and Guan, Y. (2020). lncRNA CCAT1 Acts as a MicroRNA-218 Sponge to Increase Gefitinib Resistance in NSCLC by Targeting HOXA1. Mol. Ther. Nucleic Acids *19*, 1266–1275.
9. Chen, X., Wang, Z., Tong, F., Dong, X., Wu, G., and Zhang, R. (2020). lncRNA UCA1 Promotes Gefitinib Resistance as a ceRNA to Target FOSL2 by Sponging miR-143 in Non-small Cell Lung Cancer. Mol. Ther. Nucleic Acids *19*, 643–653.
10. Chen, M., Zhuang, C., Liu, Y., Li, J., Dai, F., Xia, M., Zhan, Y., Lin, J., Chen, Z., He, A., et al. (2016). Tetracycline-inducible shRNA targeting antisense long non-coding RNA HIF1A-AS2 represses the malignant phenotypes of bladder cancer. Cancer Lett. *376*, 155–164.
11. Lin, J., Shi, Z., Yu, Z., and He, Z. (2018). LncRNA HIF1A-AS2 positively affects the progression and EMT formation of colorectal cancer through regulating miR-129-5p and DNMT3A. Biomed. & pharmacother. *98*, 433–439.
12. Guo, X., Lee, S., and Cao, P. (2019). The inhibitive effect of sh-HIF1A-AS2 on the proliferation, invasion, and pathological damage of breast cancer via targeting miR-548c-3p through regulating HIF-1α/VEGF pathway in vitro and vivo. OncoTargets Ther. *12*, 825–834.
13. Wang, Y., Zhang, G., and Han, J. (2019). HIF1A-AS2 predicts poor prognosis and regulates cell migration and invasion in triple-negative breast cancer. J. Cell. Biochem. *120*, 10513–10518.
14. Wu, R., Ruan, J., Sun, Y., Liu, M., Sha, Z., Fan, C., and Wu, Q. (2018). Long non-coding RNA HIF1A-AS2 facilitates adipose-derived stem cells (ASCs) osteogenic differentiation through miR-665/IL6 axis via PI3K/Akt signaling pathway. Stem Cell Res. Ther. *9*, 348.
15. Chen, X., Liu, M., Meng, F., Sun, B., Jin, X., and Jia, C. (2019). The long noncoding RNA HIF1A-AS2 facilitates cisplatin resistance in bladder cancer. J. Cell. Biochem. *120*, 243–252.
16. Si, J., Ma, Y., Bi, J.W., Xiong, Y., Lv, C., Li, S., Wu, N., and Yang, Y. (2019). Shisa3 brakes resistance to EGFR-TKIs in lung adenocarcinoma by suppressing cancer stem cell properties. J. Exp. Clin. Cancer Res. *38*, 481.
17. Wang, X., Peng, L., Gong, X., Zhang, X., and Sun, R. (2019). LncRNA HIF1A-AS2 promotes osteosarcoma progression by acting as a sponge of miR-129-5p. Aging *11*, 11803–11813.
18. Lu, T., Tang, J., Shrestha, B., Heath, B.R., Hong, L., Lei, Y.L., Ljungman, M., and Neamati, N. (2020). Up-regulation of hypoxia-inducible factor antisense as a novel approach to treat ovarian cancer. Theranostics *10*, 6959–6976.
19. Mineo, M., Ricklefs, F., Rooj, A.K., Lyons, S.M., Ivanov, P., Ansari, K.I., Nakano, I., Chiocca, E.A., Godlewski, J., and Bronisz, A. (2016). The Long Non-coding RNA HIF1A-AS2 Facilitates the Maintenance of Mesenchymal Glioblastoma Stem-like Cells in Hypoxic Niches. Cell Rep. *15*, 2500–2509.
20. Mu, L., Wang, Y., Su, H., Lin, Y., Sui, W., Yu, X., and Lv, Z. (2021). HIF1A-AS2 Promotes the Proliferation and Metastasis of Gastric Cancer Cells Through miR-429/PD-L1 Axis. Dig. Dis. Sci. Published online February 8, 2021. https://doi.org/10.1007/s10620-020-06819-w.
21. Xu, J., Meng, Q., Li, X., Yang, H., Xu, J., Gao, N., Sun, H., Wu, S., Familiari, G., Relucenti, M., et al. (2019). Long Noncoding RNA MIR17HG Promotes Colorectal Cancer Progression via miR-17-5p. Cancer Res. *79*, 4882–4895.
22. Yu, W., Ding, J., He, M., Chen, Y., Wang, R., Han, Z., Xing, E.Z., Zhang, C., and Yeh, S. (2019). Estrogen receptor β promotes the vasculogenic mimicry (VM) and cell invasion via altering the lncRNA-MALAT1/miR-145-5p/NEDD9 signals in lung cancer. Oncogene *38*, 1225–1238.
23. Zhu, Y., Wu, G., Yan, W., Zhan, H., and Sun, P. (2017). miR-146b-5p regulates cell growth, invasion, and metabolism by targeting PDHB in colorectal cancer. Am. J. Cancer Res. *7*, 1136–1150.
24. Li, Y., Zhang, H., Dong, Y., Fan, Y., Li, Y., Zhao, C., Wang, C., Liu, J., Li, X., Dong, M., et al. (2017). MiR-146b-5p functions as a suppressor miRNA and prognosis predictor in non-small cell lung cancer. J. Cancer *8*, 1704–1716.
25. Zhang, E., and Li, X. (2019). LncRNA SOX2-OT regulates proliferation and metastasis of nasopharyngeal carcinoma cells through miR-146b-5p/HNRNPA2B1 pathway. J. Cell. Biochem. *120*, 16575–16588.
26. Yang, E., Xue, L., Li, Z., and Yi, T. (2019). Lnc-AL445665.1-4 may be involved in the development of multiple uterine leiomyoma through interacting with miR-146b-5p. BMC Cancer *19*, 709.
27. Yeh, H.H., Lai, W.W., Chen, H.H., Liu, H.S., and Su, W.C. (2006). Autocrine IL-6-induced Stat3 activation contributes to the pathogenesis of lung adenocarcinoma and malignant pleural effusion. Oncogene *25*, 4300–4309.
28. Chang, C.H., Hsiao, C.F., Yeh, Y.M., Chang, G.C., Tsai, Y.H., Chen, Y.M., Huang, M.S., Chen, H.L., Li, Y.J., Yang, P.C., et al. (2013). Circulating interleukin-6 level is a prognostic marker for survival in advanced nonsmall cell lung cancer patients treated with chemotherapy. Int. J. Cancer *132*, 1977–1985.
29. Chang, Y.C., Su, C.Y., Chen, M.H., Chen, W.S., Chen, C.L., and Hsiao, M. (2017). Secretory RAB GTPase 3C modulates IL6-STAT3 pathway to promote colon cancer metastasis and is associated with poor prognosis. Mol. Cancer *16*, 135.
30. Taniguchi, K., and Karin, M. (2014). IL-6 and related cytokines as the critical lynchpins between inflammation and cancer. Semin. Immunol. *26*, 54–74.
31. Harada, D., Takigawa, N., and Kiura, K. (2014). The Role of STAT3 in Non-Small Cell Lung Cancer. Cancers (Basel) *6*, 708–722.